Chinese Chemical Letters 33 (2022) 3726–3732

Contents lists available at ScienceDirect

Chinese Chemical Letters

journal homepage: www.elsevier.com/locate/cclet

Rational design of a novel two-dimensional porous metal-organic framework material for efficient benzene sensor

Wenxue Zhang[a], Huiyu Ma[a], Tongtong Li[b], Cheng He[b,*]

[a] School of Materials Science and Engineering, Chang'an University, Xi'an 710064, China
[b] State Key Laboratory for Mechanical Behavior of Materials, School of Materials Science and Engineering, Xi'an Jiaotong University, Xi'an 710049, China

ARTICLE INFO

Article history:
Received 22 July 2021
Revised 26 September 2021
Accepted 1 November 2021
Available online 6 November 2021

Keywords:
Metal-organic framework material
Charge control
Sensor
Atomistix toolkit
Density functional theory

ABSTRACT

As a common volatile organic compound, benzene (C_6H_6) exists in home decoration pollution gas widely, which causes great harm to the environment and human health. Therefore, it is necessary to rationally design advanced materials with high selectivity to detect and capture C_6H_6. Herein, combined with the d-band center theory and cohesive energy, a new two-dimensional metal-organic framework material, Ni-doped hexaaminobenzene-based coordination polymer (Ni-HAB-CP) is designed, and its application potential as a C_6H_6 sensor are systematically investigated by using first principles calculation. The result shows that Ni-HAB-CP has a strong adsorption for C_6H_6 without any additional method. In addition, Ni-HAB-CP can maintain good conductivity before and after adsorption, and C_6H_6 can be easily desorbed from the surface of Ni-HAB-CP by charge control. Moreover, the *I-V* curve calculated by Atomistix Toolkit (ATK) reveals that Ni-HAB-CP has high sensitivity and selectivity to C_6H_6. Hence, Ni-HAB-CP is expected to be used as a potential material for a highly efficient and recyclable C_6H_6 sensor in the future. The calculation and analysis methods used in this paper could provide a certain theoretical basis and reference for the future research of gas sensors.

In today's highly developed human society, more and more pollution problems are accompanied with modern life. Among them, home decoration pollution has become a major killer of human health [1–3]. In addition to formaldehyde, benzene is the second largest pollutant of home decoration, it is a major reason for the increase of children with leukemia in recent years [3–6]. Because the environmental safety regulations for indoor and outdoor air quality, various industrial processes, agricultural industry and early diagnosis of diseases have become increasingly stringent in recent years, the development of effective gas and volatile organic compounds sensors has attracted great attention [7–10]. In recent years, with the continuous emergence of new technologies, there have been more and more researches on gas sensor materials [11–17]. Two-dimensional materials are widely used in gas detection because of their high specific surface area and many active sites [18–21]. Graphene is the most representative two-dimensional material, since its discovery, the application of graphene-like materials based on its structure in hazardous gas sensors has received extensive attention [22–25]. However, due to the lack of band gap of graphene, it is necessary to introduce dopants to overcome its limitations and sensitivity to a variety of harmful gasses, which increases the difficulty and cost of practical applications. Therefore, it is necessary to find efficient hazardous gas sensor materials.

Metal organic framework (MOF), is a kind of crystal material with periodic network structure formed by self-assembly of organic ligands and metals (metal ions or metal clusters) [26–28]. In recent years, due to their large specific surface area, adjustable pore size, tunable functional sites, conductivity, magnetism, ferroelectricity, luminescence and chromaticity [28,29]. According to different working principles, various MOFs have been developed, which have been widely used in the detection of a variety of gasses and volatile organic compounds [30–34]. In recent years, researchers have synthesized a new 2D transition metal organic framework material, called hexaaminobenzene-based coordination polymer (HAB-CP). Feng *et al.* have synthesized HAB-CP monomer successfully [35,36]. After a systematic and extensive exploration of the synthesis conditions, in alkaline and air environment, Ni-doped hexaaminobenzene-based coordination polymer (Ni-HAB-CP) has been prepared by the reaction of HAB linker and nickel salt in water. The difference between Ni-HAB-CP and conventional MOF materials is that 2D Ni-HAB-CP combines the advantages of porous carbon and metal organic frameworks, and thus Ni-HAB-CP has the potential as a sensor.

* Corresponding author.
E-mail address: hecheng@mail.xjtu.edu.cn (C. He).

https://doi.org/10.1016/j.cclet.2021.11.002
1001-8417/

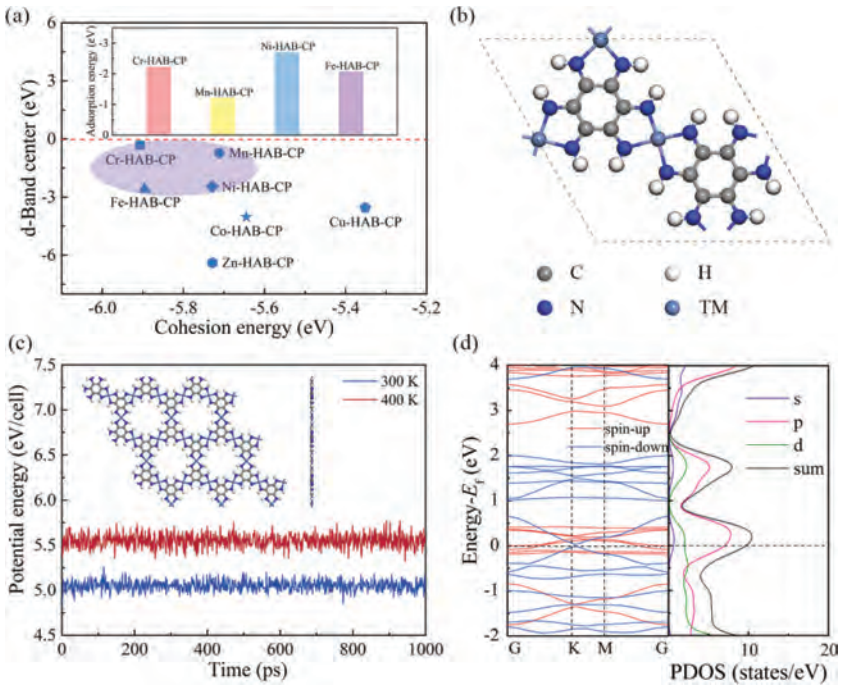

Fig. 1. (a) The Ashby plot of d-band center and cohesion energy. The light purple area represents the selected area. The illustration shows the adsorption energy of the selected material for C_6H_6. (b) The structure diagram of TM-HAB-CP. (c) The potential energy fluctuation in molecular dynamics simulation at different temperatures. (d) The energy band diagram and the density of states diagram of Ni-HAB-CP.

Based on the above-mentioned excellent characteristics, as a chemical sensor, Ni-HAB-CP has the following advantages: as a MOF material and two-dimensional material, Ni-HAB-CP provides large surface area and many active sites because of ultra-high porosity, which can accelerate the surface reaction of host and guest. Ni-HAB-CP has good reversibility for adsorption and desorption of guest molecules, which is highly renewable and recyclable. The results show that the sensing selectivity and sensitivity can be potentially improved by the adjustable pore size, shape and surface environment, and can also be changed by the introduction of functional groups in the framework. Ni-HAB-CP has high temperature stability, which is required for many practical applications. Besides, Ni-HAB-CP has been successfully prepared in the laboratory, so this study has practical significance.

In this paper, the potential of Ni-HAB-CP as a sensor material for C_6H_6 is calculated by density functional theory (DFT). The adsorption process and performance before and after adsorption of C_6H_6 and other nine small molecules on Ni-HAB-CP also be studied. The results show that Ni-HAB-CP is an excellent C_6H_6 capture material with selectivity, which has great potential as a C_6H_6 sensor material.

The computational methodology of this paper is organized as follows. Based on the first principle DFT, the atomic structure and adsorption structure of Ni-HAB-CP was optimized by using CASTEP code [37,38]. Ultra-soft pseudopotential [39] and GGA-PBE [40] exchange correlation functions were adopted. In order to avoid interaction between adjacent layers, a vacuum distance of 25 Å was used. The spin polarization was used to calculate electronic properties and adsorption energy of the structure. Van der Waals (vdW) interaction was introduced to deal with the interaction between gas molecules and Ni-HAB-CP, and DFT-D2 method [41,42] was used for semi-empirical correction. The cut-off energy was set to 400 eV, and a 4 × 4 × 1 k-point grid of Brillouin zone was adopted. The DFT + U was used on the transition metal and the value for Ni was set to 6.0 eV [43]. In order to confirm the dynamic stability of Ni-HAB-CP monomer, classical molecular dynamics (MD) simulations were performed using *NVT* [44] statistical ensemble (*V* and *T* are constants and *N* is the number of atom) and COMPASS force field [45]. And during the simulation, we chose the Andersen method [46] to control the temperature. In addition, based on DFT and non-equilibrium Green function (NEGF) method, Atomistix Toolkit (ATK) software package [47,48] was used to calculate electronic transport properties.

The corresponding calculation results are obtained by the above methods, and the analysis of results is as follows. For transition metals or structures containing transition metals, the d-band plays a key role in adsorption. The definition of d-band center is [49]: $C_d = \frac{\int_{-\infty}^{+\infty} E \times PDOS_d(E)dE}{\int_{-\infty}^{+\infty} PDOS_d(E)dE}$. The level of d-band center determines adsorption performance of materials, so it is particularly important to select structure of transition metal doped hexaaminobenzene-based coordination polymer (TM-HAB-CP) with the appropriate d-band center. The higher the d-band center, the closer to the Fermi level, the stronger the structure adsorption. The selection of TM-HAB-CP structure mainly follows the following principles: (1) Relatively high d-band center [50]; (2) high structural stability. Combined with our previous study [51], the Ashby plot between d-band center and cohesive energy can be obtained as shown in Fig. 1a. Through the above analysis, four materials in the light purple region be selected: Cr, Mn, Ni and Fe-HAB-CP. Fig. 1b shows the geometry structure of TM-HAB-CP (TM = Cr, Mn, Ni and Fe) after complete relaxation. For two-dimensional MOF material such as HAB-CP, small organic molecules are formed by substituting the hydrogen atom on the benzene ring with an amino group. The structures of TM-HAB-CP (TM = Cr, Mn, Ni and Fe) are formed by connecting small organic molecules with transition metals Cr, Mn, Ni and Fe, which are monoclinic systems. The lattice constants of TM-HAB-CP are shown in Table S1 (Supporting information). Appropriate d-band center and larger cohesive energy can ensure that the material not only has good stability, but also has good adsorption properties. In order to test the application potential of the four TM-HAB-CPs on C_6H_6 sensor materials, the adsorption energies (E_{ads}) [25] of TM-HAB-CP for C_6H_6 molecules at the same ad-

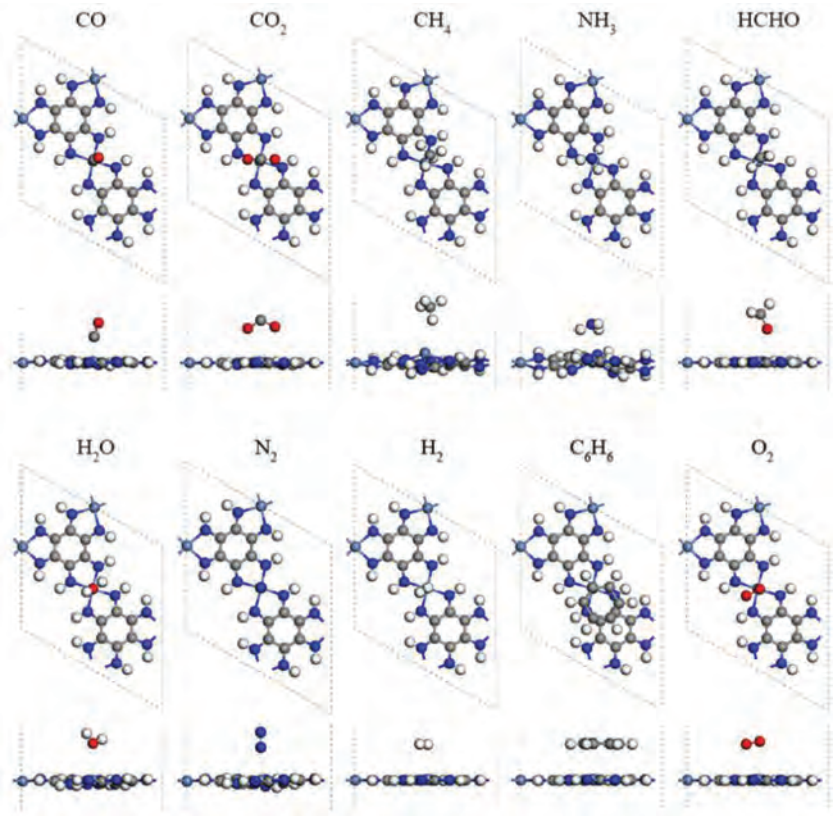

Fig. 2. The most stable adsorption configuration of Ni-HAB-CP for different gases.

sorption site were calculated by the following equation (Eq. 1):

$$E_{ads} = E_{gas/TM-HAB-CP} - E_{TM-HAB-CP} - E_{gas} \quad (1)$$

where $E_{gas/TM\text{-}HAB\text{-}CP}$, $E_{TM\text{-}HAB\text{-}CP}$ and E_{gas} represent the total energies of small molecules on TM-HAB-CP, primitive TM-HAB-CP and small molecules respectively. The more negative adsorption energy of an adsorption system indicates that the substrate has stronger capture capability to small molecules, which means adsorption effect of the substrate is better. As shown in Fig. 1a and Table S1, E_{ads} of C_6H_6 on Ni-HAB-CP is the most negative, indicating that Ni-HAB-CP has the strongest adsorption effect on C_6H_6 among the four materials. Hence, Ni-HAB-CP is chosen to analyze its application potential in C_6H_6 sensor material.

In order to verify the dynamic stability of Ni-HAB-CP, MD simulations are carried out at different temperatures (300 K, 400 K) with uniform step size of 1 fs and duration of 1000 ps. In order to minimize the confinement period, a 3 × 3 × 1 supercell with 351 atoms is constructed. Fig. 1c shows the potential energy fluctuation of Ni-HAB-CP for 1000 ps at 300 K and 400 K. It is found that the structure of Ni-HAB-CP is slightly deformed at 300 K and 400 K. There is no bond break, indicating that the structure of Ni-HAB-CP remains stable at these temperatures. In addition, the energy fluctuation with time is very small, which also proves that the structure of Ni-HAB-CP is stable at room temperature and even higher temperature. And can meet the normal the conditions of sensor use. Fig. 1d shows the band structure and density of states (DOS) of Ni-HAB-CP, and Ni-HAB-CP exhibits metallic properties. It can be predicted that this material has an excellent ability to capture some small molecules. On the other hand, the metal properties show that the adsorption properties for small molecules of Ni-HAB-CP can be controlled by charge.

In this study, the adsorption of ten different small molecules (CO, CO_2, CH_4, NH_3, HCHO, C_6H_6, O_2, H_2, H_2O and N_2) on Ni-HAB-CP are calculated firstly. Then through the size of adsorption energy and electronic properties, the adsorption performance of Ni-HAB-CP for these small molecules are discussed. In order to find the most stable adsorption structure, several different placement direction and adsorption sites are considered in the process of adsorption. The adsorption energy of all sites is calculated by Eq. 1. As shown in Fig. 2, the most stable adsorption configurations of small molecules are determined according to the calculated adsorption energy values. It can be seen that the adsorption configurations of small molecules adsorbed on Ni-HAB-CP are relatively flat except CH_4 and NH_3, which indicates that these systems are relatively stable. The corresponding E_{ads} and the minimum distance between small molecules and metals (Δd) are calculated and shown in Table 1. E_{ads} of CO, CO_2, CH_4, NH_3, HCHO, C_6H_6, O_2, H_2, H_2O and N_2 on Ni-HAB-CP are −1.241, −1.032, −1.497, −1.469, −2.086, −2.692, −5.085, −0.397, −0.547 and −1.025 eV, respectively. It can be found that E_{ads} of C_6H_6 is −2.692 eV. Such a

Table 1
Adsorption energy, minimum distance between small molecule and metal atom, charge transfer (Q_T) and work function (Φ).

Molecules	E_{ads} (eV)	Δd (Å)	Q_T (e)	Φ (eV)
CO	−1.241	2.022	−0.150	0.143
CO_2	−1.032	2.700	−0.340	0.156
CH_4	−1.497	2.683	−0.170	0.140
NH_3	−1.469	2.603	−0.030	0.145
HCHO	−2.086	2.652	−0.130	0.138
C_6H_6	−2.692	2.823	−0.110	0.142
O_2	−5.085	2.846	−0.040	0.148
H_2	−0.397	2.813	−0.030	0.141
H_2O	−0.547	3.001	−0.130	0.133
N_2	−1.025	2.600	−0.330	0.142

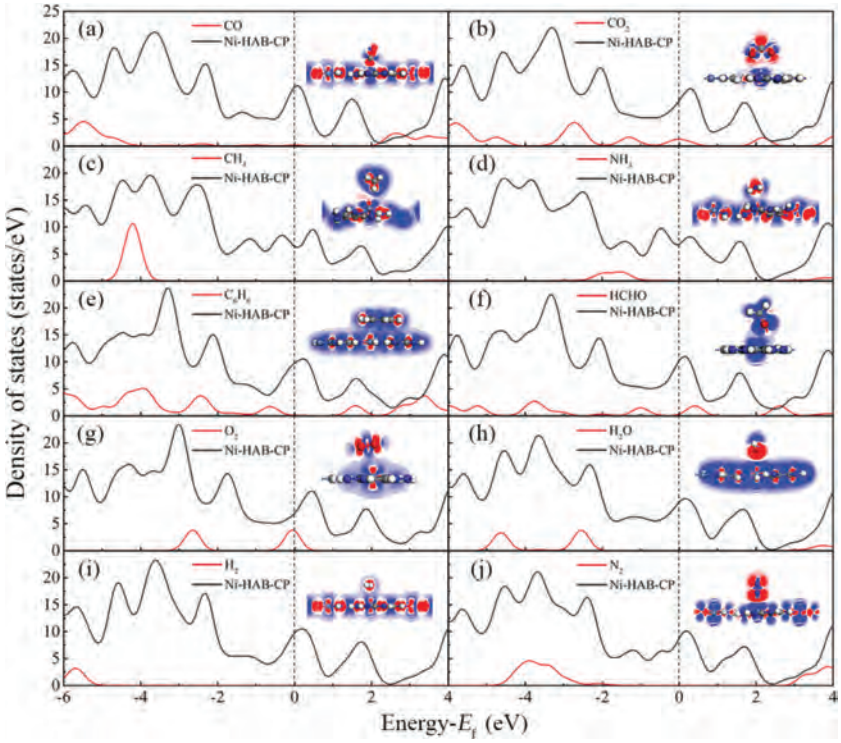

Fig. 3. The partial density of states and charge density difference of the most stable configuration of Ni-HAB-CP adsorbing different gases. Red (blue) indicates accumulation (diminishing) of electrons.

strong adsorption between Ni-HAB-CP and C_6H_6 makes Ni-HAB-CP expected to become an effective capture material for C_6H_6.

In order to analyze the electronic interaction between small gas molecules and Ni-HAB-CP, DOS and charge density difference are calculated as shown in Fig. 3. It can be seen that there is a superposition state between DOS of gas molecules and Ni-HAB-CP below Fermi energy (E_f), which can also explain the adsorption process of small molecules on Ni-HAB-CP. In addition, on the right side of DOS of C_6H_6/Ni-HAB-CP, it is obvious that the changes of the two peaks are consistent, indicating that there is a trend of chemical adsorption in this adsorption system. In order to further investigate the adsorption sensitivity of the ten small molecules on Ni-HAB-CP, the calculated charge transfer is analyzed. The insert figure on the right hand of Fig. 3 is two-dimensional section of the electron density of Ni-HAB-CP adsorbing small molecules, in which blue represents electron dissipation and red represents electron accumulation. As shown in Fig. 3, electron dissipation exists in most of the small molecules and the surface of Ni-HAB-CP. From this point of view, the greater electron dissipation between small molecules and Ni-HAB-CP, the stronger interaction between the two substances. It approves that Ni-HAB-CP could adsorb small molecules to a certain extent.

According to the above discussion and analysis, Ni-HAB-CP is expected to be an effective capture material for C_6H_6. The gas sensitivity of Ni-HAB-CP to C_6H_6 is discussed in this part. However, from the perspective of E_{ads} of single molecule, E_{ads} of Ni-HAB-CP for O_2 (−5.085 eV) is greater than E_{ads} of Ni-HAB-CP for C_6H_6 (−2.692 eV). However, air is a mixed gas. Therefore, before discussing the gas sensitivity of Ni-HAB-CP to C_6H_6, the co-adsorption of O_2 and C_6H_6 on Ni-HAB-CP should be discussed firstly. As shown in Fig. S1 (Supporting information), it is a schematic diagram of the energy barrier that two small molecules need to cross when O_2 and C_6H_6 are co-adsorbed on Ni-HAB-CP. It can be seen clearly that in this situation: the energy barrier which needs to ~~be~~ overcome for C_6H_6 desorption is 0.168 eV, while for O_2, the energy barrier is 0.117 eV Therefore, the adsorption of O_2 on Ni-HAB-CP will not affect the study of gas sensitivity of Ni-HAB-CP to C_6H_6.

Extraordinary gas sensor materials not only have high adsorption capacity for target molecules, but also need excellent conductivity. Thus, it is necessary to calculate the electron transport properties and compare the changes of electronic properties before and after adsorption of C_6H_6. In order to reasonably evaluate the quantum transport, the quantum conduction (G) function of the adsorption system is determined by the following formula (Eq. 2) [52]:

$$G = G_0 \sum_{i=1}^{M} T_i \quad (2)$$

where, $G_0 = 2e^2/h$ (e is the electron quantity, h is the Planck constant), T_i is the transmission probability of the i th channel, and M is the number of propagating modes passing through E_f. Without considering the scattering, T_i is unit 1. According to the formula, the more band passing through Fermi, the better conduction effect. Fig. S2 (Supporting information) shows the calculated results of DOS of Ni-HAB-CP before and after adsorption of C_6H_6 and G according to Eq. 2. It can be seen that G value of Ni-HAB-CP before and after adsorption of C_6H_6 is not zero, which indicates that the conductivity of Ni-HAB-CP does not change greatly before and after adsorbed C_6H_6 molecule. The following diagram of DOS also can confirm this result to a certain extent. Because the system is still a conductor after adsorbed C_6H_6, it is still easy to introduce electrons into the whole system after adsorption. Thus, the adsorption capacity of Ni-HAB-CP for C_6H_6 can be controlled by injecting charge.

In order to practice Ni-HAB-CP as a C_6H_6 sensor with reusable performance in actual application, the adsorption and desorption process of C_6H_6 on Ni-HAB-CP needs to be further explored. From the above analysis of G and DOS before and after adsorption, the adsorption capacity of Ni-HAB-CP for C_6H_6 can be controlled by injecting charge in the experiment. Therefore, the change of adsorption energy of Ni-HAB-CP for C_6H_6 after different charge injection should be discussed in our following study. As shown in Fig. 4a,

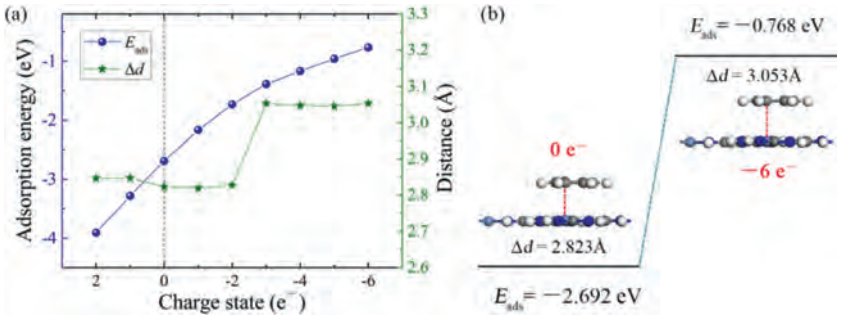

Fig. 4. (a) Relationship between E_{ads} and Δd of C_6H_6 adsorbed on Ni-HAB-CP and amount of injected charge. (b) The adsorption configuration diagram without charge injected and with six negative charges injected.

E_{ads} tends to be more and more negative with the increase of injected positive charges, which indicates that the positive charge injection could not desorb C_6H_6 from Ni-HAB-CP surface; on the contrary, with the increasing the number of injected negative charges, the absolute value of E_{ads} becomes smaller and smaller until $|E_{ads}| < 1$. This shows that the interaction force of C_6H_6 on Ni-HAB-CP surface becomes smaller and smaller due to the negative charge injection. Some literatures have shown that when $|E_{ads}| < 1$, it can be considered that the adsorption between small molecules and adsorbents is very weak and negligible [53]. Then, C_6H_6 molecule is manually moved to the position 3 Å away from the Ni atom in order to weaken the intermolecular interaction of the original system after the injection of charge. As shown in Fig. 4a, the minimum distance (Δd) between the small molecule and the metal atom increases significantly and is greater than 3 Å after the injection of three negative charges. Some literatures have shown that when $\Delta d > 3$ Å, it can be considered that the adsorption between small molecules and adsorbents is very weak and could be ignored. Fig. 4b shows the adsorption configuration diagram without charge injected and with six negative charges injected. The changes of E_{ads} and Δd can be seen more clearly: E_{ads} is changed significantly from −2.692 eV to −0.768 eV, and Δd is increased from 2.823 Å to 3.053 Å The interaction between Ni-HAB-CP and C_6H_6 decreases with the increase of injected negative charges. Considering E_{ads} and Δd of C_6H_6/Ni-HAB-CP adsorption system after charge injection, we can conclude that the injection of more than five negative charges could desorb C_6H_6 from Ni-HAB-CP surface. In other words, Ni-HAB-CP could be reused as a C_6H_6 sensor by applying a certain amount of negative charge.

In order to quantitatively analyze whether Ni-HAB-CP can successfully detect C_6H_6 molecules in air as a sensing material, based on NEGF method, the *I-V* curves of Ni-HAB-CP before and after adsorption of C_6H_6 at 300 K are simulated and analyzed. Due to the aeolotropism of the system, the X and Y directions are studied respectively. As shown in Fig. S3 (Supporting information), it's the schematic diagram and *I-V* curve of Ni-HAB-CP and C_6H_6/Ni-HAB-CP system in X direction. It can be known that the change of *I-V* curve obtained by applying voltage in the X direction is not obvious, so the result of X direction will not be discussed in depth here. The position of applying bias voltage in the Y direction to Ni-HAB-CP and different adsorption systems (C_6H_6/Ni-HAB-CP adsorption system is taken as an example here) are shown respectively (Figs. 5a and b). The calculated *I-V* curves are shown in Figs. 5c and d. For C_6H_6, the current passing through C_6H_6/Ni-HAB-CP system is significantly less than that passing through Ni-HAB-CP system under the same voltage. When the voltage is between 0.5 V and 1.5 V, there is a change that can be observed clearly. When the voltage is 0.51 V, the current through Ni-HAB-CP is about 22.9 μA. After adsorption of C_6H_6, the current is about 4.1 μA under the same bias voltage, which decreases 82.1%, indicating the resistance increases after adsorption. When the applied voltage is 1.5 V, the differences between different systems can be observed more clearly. In addition to the ATK, the optical changes before and after adsorption of C_6H_6 also were calculated. The results showed that there was no obvious change in the absorption peaks in the infrared and visible regions before and after adsorption. As shown in Fig. S4 (Supporting information), compared with the structure before adsorption, the system after adsorption of C_6H_6 shows more obvious light absorption in the ultraviolet range. The change of optical absorption peak indicates that Ni-HAB-CP is sensitive to C_6H_6. Therefore, in practical application, because of the change of resistance before and after Ni-HAB-CP adsorbs C_6H_6 molecules (C_6H_6/Ni-HAB-CP > Ni-HAB-CP), the existence of C_6H_6 can be detected directly. Compared with other adsorption systems and C_6H_6/Ni-HAB-CP system, the current of them is not equal at the same voltage, which indicates that Ni-HAB-CP is sensitive and selective for C_6H_6. The mechanism of chemical resistance sensor is mainly attributed to the adsorption of gas molecules on sensing materials, which causes the transfer of electrons and holes. Or the reaction of gas molecules on the surface of the functional material, which causes the change in resistance (or conductance) of the sensing materials [30]. From the charge transfer in Table 1, it can be seen that there is a clear transfer of 0.11 e from Ni-HAB-CP monomer to C_6H_6 molecule. It can also be seen from Fig. 5 that after adsorption of C_6H_6, the resistance of Ni-HAB-CP also changes significantly. Therefore, we believe that Ni-HAB-CP has large potential as a chemical resistance C_6H_6 sensor.

Through the previous research, it can be concluded that under certain external force (injecting a certain amount of negative charge into the system), Ni-HAB-CP has good reversibility for the adsorption and desorption of C_6H_6 molecule, which makes it have certain renewability and recyclability as potential material of C_6H_6 sensor. However, without injecting charge into C_6H_6/Ni-HAB-CP system to make C_6H_6 desorb from Ni-HAB-CP surface, how is the capacity of Ni-HAB-CP captures C_6H_6? It is worth discussing. Therefore, in order to evaluate the ability of Ni-HAB-CP captures C_6H_6, the number of C_6H_6 that Ni-HAB-CP can capture is discussed in this part. E_{ads} of the adsorption system for multiple (≥ 2) C_6H_6 molecules is determined by the following equation (Eq. 3):

$$E_{ads} = nE_{gas/Ni-HAB-CP} - (n-1)E_{gas/Ni-HAB-CP} - E_{gas} \quad (3)$$

where n ($n \geq 2$) represents the adsorption system adsorbs to the n-th C_6H_6 molecule, and other expressions are consistent with Eq. 1. Here, all the possible adsorption sites of multi-C_6H_6 adsorbed on Ni-HAB-CP are considered. The most stable adsorption configuration by whether the adsorption system is deformed and E_{ads} are also determined. As shown in Fig. S5 (Supporting information), the relationship between adsorption energy and charge transfer of Ni-HAB-CP adsorbs C_6H_6 with adsorption quantity and the most stable adsorption configuration are illustrated. It can be seen that

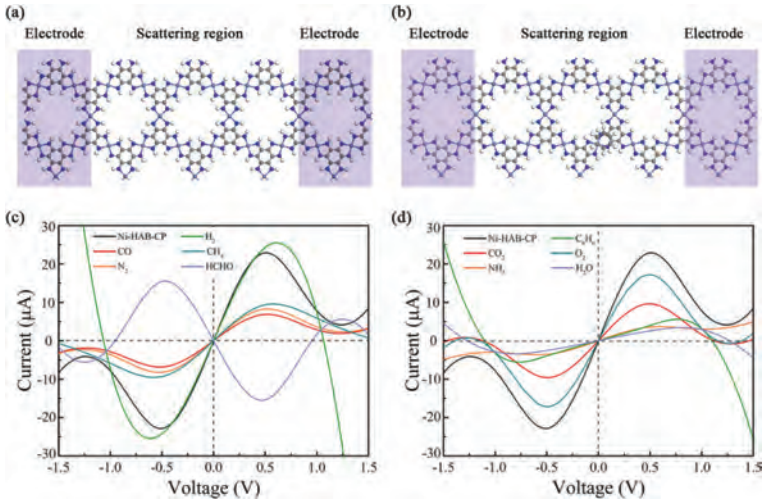

Fig. 5. The schematic diagram (a, b) and *I-V* curve (c, d) of Ni-HAB-CP before and after adsorption of small molecules in Y direction.

the amount of charge transfer (negative sign represents the direction of charge transfer, not the size) increases with the increase of the amount of C_6H_6 adsorbed by Ni-HAB-CP. In general, $|E_{ads}|$ decreases with the increase of the amount of C_6H_6 adsorbed on Ni-HAB-CP. Considering that too much small molecules adsorbed on the same layer will lead to large interaction force, therefore, there are two kinds of adsorption ideas when adsorbing the fifth C_6H_6 molecule: The first is the molecule still adsorbed on the same layer, and the other is the molecule adsorbed on the second layer of Ni-HAB-CP. As shown in Fig. S5, $|E_{ads}|$ of the second layer adsorption on the Ni-HAB-CP surface increases rather than decreases, which indicates that this kind of adsorption configuration makes the molecules in the system have greater interaction force. Therefore, it doesnot be considered. While compared with the system of adsorbing four C_6H_6 molecules, the decline of $|E_{ads}|$ of adsorbing the fifth C_6H_6 molecule on the same layer is not obvious (the adsorption of the sixth small molecule is the same as above, which is not repeated here). Thus, Ni-HAB-CP can completely adsorb four C_6H_6 molecules with stable configuration. Therefore, in addition to injecting a certain amount of negative charge into the system, Ni-HAB-CP is also a candidate for high capacity C_6H_6 capture material.

In this paper, taking search of suitable materials and adsorption properties as the starting and main line, the structural stability and electrical properties of different small molecules (CO, CO_2, CH_4, NH_3, HCHO, C_6H_6, O_2, H_2, H_2O and N_2) adsorbed on Ni-HAB-CP are investigated by using first principles calculation. E_{ads} of C_6H_6 on Ni-HAB-CP is −2.692 eV, which indicates that Ni-HAB-CP has a strong adsorption capability for C_6H_6 and is expected to be an effective C_6H_6 capture material. When 5 (or > 5) negative charges are injected into C_6H_6/Ni-HAB-CP adsorption system, $|E_{ads}|$ of the system is less than 1. The results reveal that C_6H_6 can be desorbed from Ni-HAB-CP surface by a certain amount of negative charge injection. From the *I-V* curve, when the voltage is ~0.51 V, the current through the C_6H_6/Ni-HAB-CP system is 82.1%, which is lower than the current through the Ni-HAB-CP system under the same bias voltage, indicating that the resistance of the system increases after adsorption. The results reveal that Ni-HAB-CP has high sensitivity and selectivity to C_6H_6, and the detection of C_6H_6 can be transmitted by electrical signal. Therefore, Ni-HAB-CP can be used as a potential recyclable C_6H_6 sensor material. In additian, Ni-HAB-CP can completely adsorb four C_6H_6 molecules with stable configuration, the calculated result indicates that Ni-HAB-CP is also a candidate for high capacity C_6H_6 capture material without any additional method.

Declaration of competing interest

The authors declare that they have no known competing financial interests or personal relationships that could have appeared to influence the work reported in this paper.

Acknowledgments

The authors acknowledge supports by National Natural Science Foundation of China (No. 51471124 and U1766216), National Key R&D Program of China (No. 2018YFB0905600) and Natural Science Foundation of Shaanxi Province, China (Nos. 2019JM-189 and 2020JM-218), the Fundamental Research Funds for the Central Universities (No. CHD300102311405), HPC platform, Xi'an Jiaotong University.

Supplementary materials

Supplementary material associated with this article can be found, in the online version, at doi:10.1016/j.cclet.2021.11.002.

References

[1] P. Wu, X.J. Jin, Y.C. Qiu, D.Q. Ye, Environ. Sci. Technol. 55 (2021) 4268–4286.
[2] P. Wu, S. Zhao, J. Yu, et al., ACS Appl. Mater. Interfaces 12 (2020) 50566–50572.
[3] W.L. Li, Q.G. Jiang, D.D. Li, Z.M. Ao, T.C. An, Chin. Chem. Lett. 32 (2021) 2803–2806.
[4] J. Cui, Y. Zhao, M. Wang, S. Wang, J. Ma, Chin. Chem. Lett. 31 (2020) 779–782.
[5] S. Kang, M. Wang, N. Zhu, et al., Chin. Chem. Lett. 30 (2019) 1450–1454.
[6] S.C. Kim, W.G. Shim, Appl. Catal. B: Environ. 92 (2009) 429–436.
[7] O.S. Wenger, Chem. Rev. 113 (2013) 3686–3733.
[8] B. Wang, X.S. Dong, Z. Wang, Y.F. Wang, Z.Y. Hou, ACS Sens. 5 (2020) 994–1001.
[9] H. Wang, W.P. Lustig, J. Li, Chem. Soc. Rev. 47 (2018) 4729–4756.
[10] H. Lin, M. Jang, K.S. Suslick, J. Am. Chem. Soc. 133 (2011) 16786–16789.
[11] J. Shu, Z.L. Qiu, D.P. Tang, Anal. Chem. 90 (2018) 9691–9694.
[12] T. Kawano, H.C. Chiamori, M. Suter, et al., Nano Lett. 7 (2007) 3686–3690.
[13] J. Shu, Z.L. Qiu, Q. Zhou, D.P. Tang, Chem. Commun. 55 (2019) 3262.
[14] J.R. Stetter, J. Li, Chem. Rev. 108 (2008) 352–366.
[15] L. Tang, P. Xu, M. Li, H. Yu, X. Li, Chin. Chem. Lett. 31 (2020) 2155–2158.
[16] H.Y. Yang, C.Z. He, L. Fu, et al., Chin. Chem. Lett. 32 (2021) 3202–3206.
[17] E.D. Xing, L.Q. Liang, Y.J. Dong, W.M. Huang, Chin. Chem. Lett. 26 (2015) 1322–1326.
[18] R. Wang, C.Z. He, W.X. Chen, C.X. Zhao, J.R. Huo, Chin. Chem. Lett. 32 (2021) 3821–3824.
[19] J.D. Fowler, M.J. Allen, V.C. Tung, et al., ACS Nano 3 (2009) 301–306.
[20] L. Fu, R. Wang, C.X. Zhao, et al., Chem. Eng. J. 414 (2021) 128857.
[21] J. Shu, Z.L. Qiu, S.Z. Lv, K.Y. Zhang, D.P. Tang, Anal. Chem. 89 (2017) 11135–11142.
[22] S.M. Aghaei, A. Aasi, S. Farhangdoust, B. Panchapakesan, Appl. Surf. Sci. 536 (2021) 147756.
[23] L. Chen, Z. Xiong, Y. Cui, H. Luo, Y. Gao, Appl. Surf. Sci. 542 (2021) 148767.
[24] C. He, M. Zhang, T.T. Li, W.X. Zhang, Appl. Surf. Sci. 505 (2020) 144619.

[25] C. He, M. Zhang, T.T. Li, W.X. Zhang, J. Mater. Chem. C 8 (2020) 6542–6551.
[26] H. Furukawa, K.E. Cordova, M. O'Keeffe, O.M. Yaghi, Science 341 (2013) 974.
[27] H. Liu, Y. Wang, Z. Qin, et al., J. Phys. Chem. Lett. 12 (2021) 1612–1630.
[28] Y.T. Qin, Y. Wan, J. Guo, M.T. Zhao, Chin. Chem. Lett. 33 (2022) 693–702.
[29] H. Deng, S. Grunder, K.E. Cordova, et al., Science 336 (2012) 1018–1023.
[30] H.Y. Li, S.N. Zhao, S.Q. Zang, J. Li, Chem. Soc. Rev. 49 (2020) 6364–6401.
[31] W.P. Lustig, S. Mukherjee, N.D. Rudd, et al., Chem. Soc. Rev. 46 (2017) 3242–3285.
[32] K. Chen, C. Wu, Chin. Chem. Lett. 29 (2018) 823–826.
[33] H.K. Li, H.L. Ye, X.X. Zhao, et al., Chin. Chem. Lett. 32 (2021) 2851–2855.
[34] H. Wang, X. Wang, R.M. Kong, L. Xia, F. Qu, Chin. Chem. Lett. 32 (2021) 198–202.
[35] N. Lahiri, N. Lotfizadeh, R. Tsuchikawa, V.V. Deshpande, J. Louie, J. Am. Chem. Soc. 139 (2017) 19–22.
[36] D. Feng, T. Lei, M.R. Lukatskaya, et al., Nat. Energy 3 (2018) 30–36.
[37] M.D. Segall, P.J.D. Lindan, M.J. Probert, et al., J. Phys.: Condens. Matter 14 (2002) 2717–2744.
[38] S.J. Clark, M.D. Segall, C.J. Pickard, et al., Z. Kristallogr. 220 (2005) 567–570.
[39] D. Vanderbilt, Phys. Rev. B 41 (1990) 7892–7895.
[40] J.P. Perdew, K. Burke, M. Ernzerhof, Phys. Rev. Lett. 78 (1997) 1396.
[41] S. Grimme, J. Comput. Chem. 25 (2004) 1463–1473.
[42] S. Grimme, S. Ehrlich, L. Goerigk, J. Comput. Chem. 32 (2011) 1456–1465.
[43] F. Zhou, M. Cococcioni, C.A. Marianetti, D. Morgan, G. Ceder, Phys. Rev. B 70 (2004) 235121.
[44] F. Ding, A. Rosen, K. Bolton, Phys. Rev. B 70 (2004) 075416.
[45] H. Sun, J. Phys. Chem. B 102 (1998) 7338–7364.
[46] H.C. Andersen, J. Chem. Phys. 72 (1980) 2384–2393.
[47] M. Brandbyge, J.L. Mozos, P. Ordejon, J. Taylor, K. Stokbro, Phys. Rev. B 65 (2002) 165401.
[48] J. Taylor, H. Guo, J. Wang, Phys. Rev. B 63 (2001) 13.
[49] W. Zhang, D. Cheng, J. Zhu, RSC Adv. 4 (2014) 42554–42561.
[50] G. Gao, E.R. Waclawik, A. Du, J. Catal. 352 (2017) 579–585.
[51] T.T. Li, C. He, W.X. Zhang, Energy Storage Mater. 25 (2020) 866–875.
[52] C. He, G. Liu, W.X. Zhang, Z.Q. Shi, S.L. Zhou, RSC Adv. 5 (2015) 22463–22470.
[53] V. Kumar, D. Azhikodan, D.R. Roy, J. Hazard. Mater. 405 (2021) 124168.